Electrostatic powder attraction for the development of a novel recoating system for metal powder bed-based additive manufacturing

Julia Foerster [a,*], Marco Michatz [a], Maximilian Binder [a], Alexander Frey [b], Christian Seidel [a,c], Georg Schlick [a], Johannes Schilp [a,d]

[a] Fraunhofer Institute for Casting, Composite and Processing Technology IGCV, Augsburg, Germany
[b] University of Applied Sciences Augsburg, Electrical Engineering Faculty, Augsburg, Germany
[c] University of Applied Sciences Munich, Department for Mechatronics and Applied Sciences, Munich, Germany
[d] University of Augsburg, Chair of Digital Manufacturing, Augsburg, Germany

1. Introduction

The increasing industrial relevance of powder bed-based additive manufacturing has led to new technological trends across industries in recent years. Powder bed-based processes are characterized in particular by near-net-shape component production with geometric design freedom. In these processes, components are manufactured based on digital design models through the interplay of the layer-by-layer powder application and targeted material consolidation. Powder bed fusion of metals using a laser beam (PBF-LB/M) is the most widely used process for the production of metallic components with built part densities approaching 100% [1]. The focus of current technology developments includes the processing of different powder materials in one manufacturing process (so-called multi-material process) [2–4] and the increase of powder efficiency [1,5]. In order to implement these approaches, improvements in flexibilization of powder application systems are necessary.

An approach is offered by a high resolution powder application which emerged from electrophotography (EP). This powder application principle operates without contact and is based on the attraction of electrical charges with electrostatic fields. The process has been established for years in laser printers and photocopiers for transporting dry solid particles. In perspective, EP powder application in powder bed-based additive processes is possible, similar to a laser printer, independent of the powder flowability with simultaneous high local resolution and high application speed [6]. An electrophotographic powder application module (EPAMO) describes a mechanical system for picking up, transporting and depositing powder particles in environmental conditions of a powder bed-based additive manufacturing system. Previous research on the integration of an EPAMO into powder bed-based processes has primarily focused on the processing of polymer powders [7–9]. Boivie et al. investigated the electrophotographic application of metal and ceramic powders for additive manufacturing purposes in the metal printing process [9–11]. However, the transferability of the process and components to a PBF-LB/M process has not yet been fully addressed [12,13]. The objective of this paper is to enable a prototype to attract a typical PBF-LB/M metal powder and to investigate imaging (exposure) for the selective powder attraction with the perspective of implementation in a PBF-LB/M system.

First, current challenges of powder application in powder bed-based additive manufacturing are presented, as well as the principles of electrophotography, which can help to avoid the obstacles in processing powders of different materials (multi-material) [14] and shapes (spherical and non-spherical particles) [15] as well as in flexibilization

* Corresponding author.
E-mail address: julia.foerster@igcv.fraunhofer.de (J. Foerster).

of the recoating systems (full-area and selective deposition) [2]. In order to transfer the powder attraction of electrophotography to PBF-LB/M, a full-surface attraction to of metal powder the photoconductor was modeled. Parameters derived from this were validated experimentally. Further, selective attraction is presented by testing diodes for exposure. Based on this, an influence analysis and optimization of selected process parameters was performed.

1.1. Challenges of powder application in powder bed-based additive manufacturing

Established, conventional powder application systems that focus on leveling the powder bed are based on mechanical, contact-based mechanisms such as a flat squeegee mechanism with a blade or roller [16]. Those powder application systems are dependent on the quality of the powders due to their contact-based mode of action. PBF-LB/M-typical powders are primarily characterized by a high flowability due to spherical particles and a specific, narrow particle size distribution (PSD). The production of such powders is cost-intensive and an obstacle to the expansion of the process range and application, e.g. in series production. Exploiting a broader PSD as well as processing non-spherical particles can make powder bed-based additive manufacturing not only more resource-efficient but also more economically viable. However, powders with these attributes often exhibit low flowability. This leads to errors in layer generation during application with conventional mechanisms and thus reduce component quality [15].

Multi-material processing presents a particular challenge for powder application since several powders have to be applied in one process. Previous systems require either the targeted sequential removal of the applied powder or a selective application. The multi-material systems available to date are based on the modification of conventional mechanisms. They are therefore also subject to their restrictions and depend on the powder quality. A direct, arbitrary change of the layer generation with high resolution and homogeneous layer in suitable thickness is still under research [14,17–19]. A first approach to integrate the EP process phases into the PBF-LB/M is currently being carried out at Fraunhofer Institute for Casting, Composite and Processing Technology (IGCV) [12,13,20]. Using a translational principle device (stamp principle), it can be shown that an organic (O) photoconductor (PC) can be charged under thermal and atmospheric conditions as in an PBF-LB/M system [12,13]. Based on these investigations, the process is extended in this paper to include full-area and selective powder attraction.

1.2. Relevant principles of electrophotography

Powder application by EP represents a novel approach for PBF-LB/M to equally counteract the existing limitations due to the application method as well as the dependence on the flowability of conventional mechanisms in a layer application process. The EP application principle is based on targeted electrostatic mass transport and thus acts in a non-contact manner. The conventional EP process consists of six phases [21,22,23]. First, an electrostatic field is homogeneously applied to a PC's surface (phase 1). The PC is a light-sensitive component that becomes locally conductive when exposed to incident photons. The field can be selectively neutralized by exposing the charged PC to light due to the interaction with the photons (imaging, phase 2). When a photon strikes the appropriately doped region of the charged PC, so-called electron--hole pairs can be generated if sufficient energy is available [24]. The underlying physical effect is the internal photoelectric effect [25]. This process leads to a latent charge pattern on the PC's surface and is schematically shown in a longitudinal view of the PC in Fig. 1. The pairs separate according to the external field (E_{outer} in Fig. 1) and migrate according to their charge either into the grounded carrier material or neutralize the charges at the surface. Only with the subsequent attraction of particles (development, phase 3), the desired image becomes visible according to the given layer and exposure information. Deposition of the powder (transfer, phase 4) completes the essential powder application process [23,24]. This is followed by thermal fixation of the powder loosely adhering to the paper (phase 5). Cleaning and discharging (phase 6) is a necessity to prepare the PC for the next cycle. The residual powder, as well as charges, are removed so that the PC is reset to its neutral state [22,23,26].

2. Electrostatic modeling of field-induced attraction of particles between photoconductor and powder storage

This chapter investigates the possibility of attracting powder layers from a bulk powder storage with electrostatic fields. In an approximation, the field forces at which it is possible to attract powder particles are estimated. The fringing fields of the designed components are also considered. These preliminary considerations result in parameter combinations for the tests and thus form the basis for the series of experiments. The actual three-dimensional geometry of the process modules involved in the attraction experi-ments represent the modeling foundation [20]. Results of the occurring field formation during the process of attraction are visualized in Fig. 2. The model includes the carrier with the attached OPC and the attraction plate for powder storage

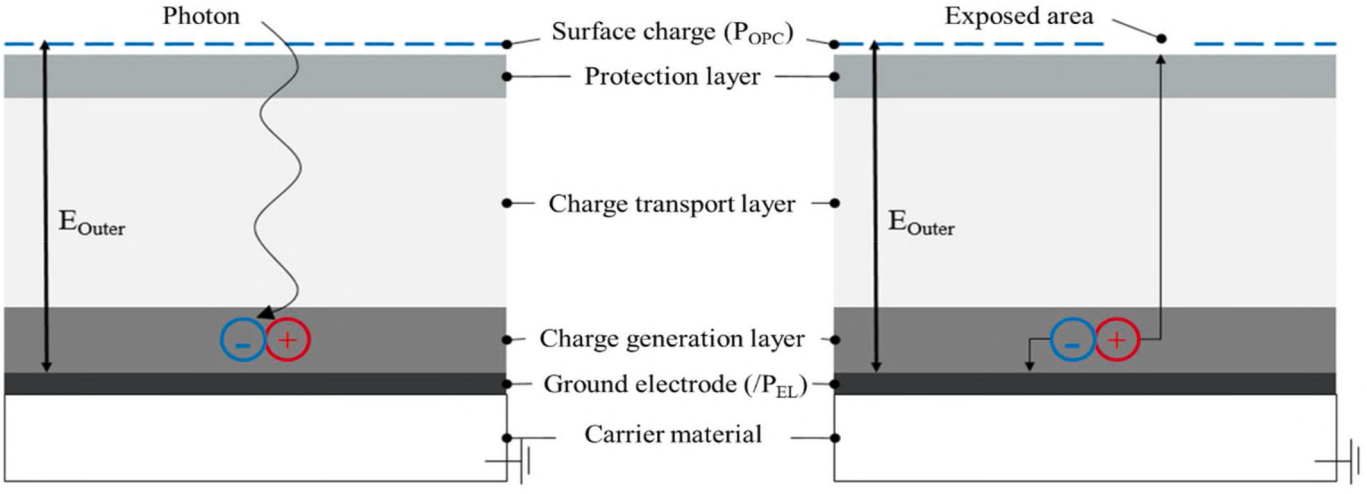

Fig. 1. Schematic illustration of charge generation (left) and neutralization (right) as a longitudinal view of a photoconductor with the surface potential (P_{OPC}) and the ground electrode respectively (if connected) the potential of the photoconductor's electrode (P_{EL}), following [21].

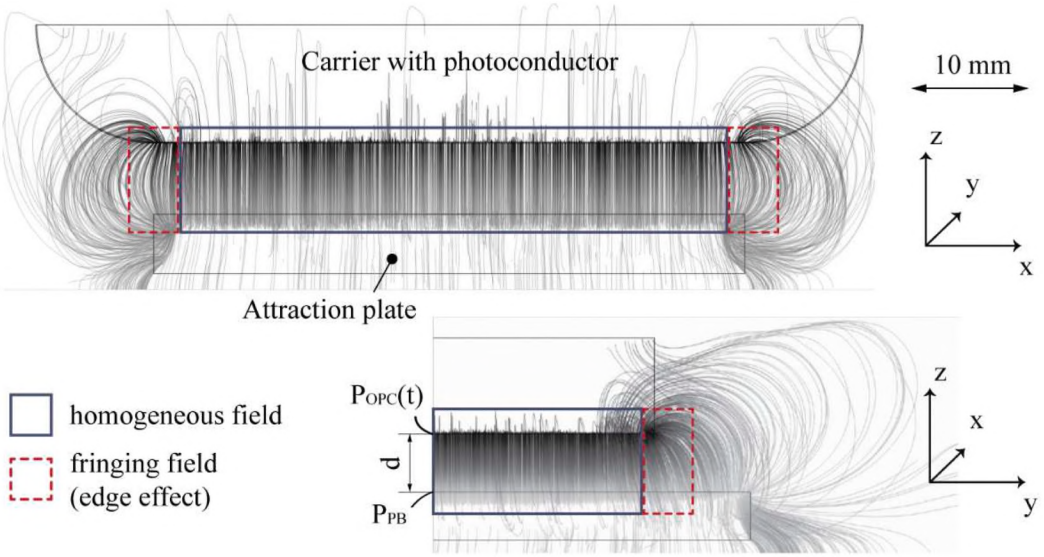

Fig. 2. Visualization of the field characteristic between photoconductor and the attraction plate with the time depending surface potential of the photoconductor ($P_{OPC}(t)$), the potential of the powder bed (P_{PB}) and the distance (d) between them.

surrounded by the process gas. No powder is modeled for the general determination of the field force and in particular the edge effects as a result of the fringing field (cf. Fig. 2).

The electrostatic phenomena in the modeling domains are described by Gauss's law $\nabla \cdot D = \rho_v$ with the dimension depending electric displacement field D and the volume charge density ρ_v. The linear constitutive media relation $D = E \cdot \varepsilon_0 \cdot \varepsilon_r$ is used with the assumption of an irrational (curl free) field where E is the electric field and $\varepsilon = \varepsilon_0 \cdot \varepsilon_r$ defines the dielectric media constants. The field characteristic suggests that the edge effects can hinder the interference-free powder attraction close to the edges. However, these specific edge effects can be reduced to some degree with the use of radii and in particular by enlarging the surface from the carrier or the attraction plate while keeping the useable area for attraction fixed [20]. With this consideration, a homogeneous field in the attraction region can be assumed for practice, thus the analytical capacitance model in Fig. 3 is considered to be sufficient for further calculations.

In the model, the field calculation was extended by an approximation of the powder layer to be attracted. Since only the uppermost particles of the powder layer can be attracted by the PC, the focus of the calculation was set on the static field E_{gas} in the gap between the powder layer and the PC with the effective distance of the particles surface to the PC's surface of 0.8 mm. The applied powder layer shifts the relevant potential (P_{PB}) and the field determination from the attraction plate to the powder surface due to the strongly differing permittivity compared to the process gas. The charge induction in the powder takes place via a contact charge through the powder attraction plate, which is set up in an isolated arrangement. For now it cannot be exclusively proven which mechanism (e.g. charge induction or tribological charging) defines the charge transport. For an estimation of the necessary field for powder attraction, the powder layer is treated as a dielectric in the calculation.

A capacitor assembly was set up to determine an approximate permittivity value for the metal powder. Two aluminum electrodes with a diameter of 24 mm were placed in parallel at a distance of 1.1 mm from each other forming a capacitor. A capacitance meter (ELV DCM 7001) was connected several times for 24 h to determine the maximum achievable capacitance in the RC element. First, the air gap between the electrodes was measured yielding 5,71 pF. Then the air gap was filled with the steel powder of 20MnCr5 (PSD between 25 µm and 71 µm, monomodal, produced by gas atomization) with identical distances and sealed edges yielding up to 320 pF. The described measurement was replicated in a simulative study to assess validity. Within the study 6.15 pF were calculated for the air gap. The existing residual error is due to the simplifying measures of the calculations and the basic measurement scheme but is considered to be sufficiently low to provide a guide value of the permittivity. For the powder measurement of 320 pF, the permittivity was varied in the study until the calculated permittivity value coincided with the measured one. Taking into account the possible error, a maximum permittivity ε_{powd} of 90 is conceivable.

With the assumption of a process gas, the field force in the gap can be approximated and compared to the minimum required field $E_{min,att}$ for attraction with $E_{att}=E_{gas}+E_{powd}$. $E_{min,att}$ is an estimation if, in theory,

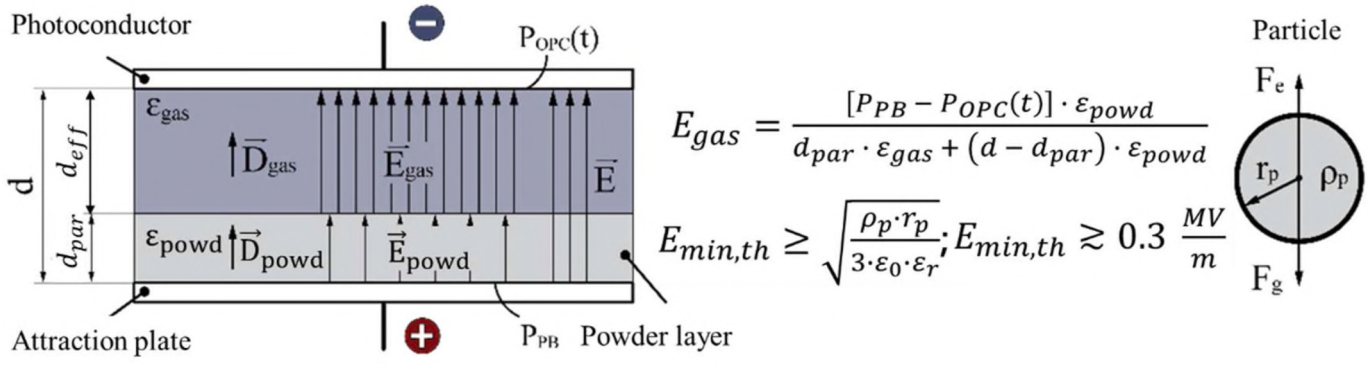

Fig. 3. Approximation of the powder attraction with a powder layer.

electrostatic mass transport is possible within a given charge and mass of the particle [7]. E_{att} is formed with the balance of forces $F_g \leq F_e$ or $m_p \cdot g \leq Q_p \cdot E_{att}$ using the maximum surface charge $Q_p = E_{breakdown} \cdot 4\pi \cdot \varepsilon_0 \cdot \varepsilon_r \cdot r_p^2$ that can be sustained by the particle in the process gas considering the electrical breakdown field limit $E_{breakdown}$ for the gas with r_p the particle radius (depending on the PSD), $\varepsilon = \varepsilon_0 \cdot \varepsilon_r$ the dielectric constants. The particle weight force $m_p = \frac{4}{3} \cdot \rho_p \cdot \pi \cdot r_p^3$ assumes spherical particles with ρ_p the particle density, and g the gravity acceleration. With the metal powder used $E_{min,att}$ is at least 0.3 MV/m with the maximum possible particle charge under air atmosphere. However, the particle charge caused by the attraction, for example by friction effects, can never be assumed to be perfectly given. It is therefore possible that E_{lift} may have to be significantly higher. Furthermore, it is known that when a particle is lifted from a substrate, electric field forces such as the electric imaging force between the particle charges and their imaging forces and surface forces (such as the van der Waals force) act in addition to the Coulomb forces [27] which will further increase the given $E_{min,\ att}$ estimation. This field comparison nevertheless establishes a theoretical basis for the experiments shown below, provides indications for useful parameter combinations and adds an estimate on the feasibility with regard to the breakdown voltage of the process gas.

3. Experimental setup and experiment procedure for selective attraction

To gain insight and generate results on the attraction of metal powder, an experimental test setup (see Fig. 4) was developed and is explained below. This research activity aimed to attract and transport metal powders via an OPC adapted from electrophotography. OPCs are the most widely used and technically developed material in EP [22]. Due to the moderate ambient temperature of a maximum of 60 °C in the build chamber of a PBF-LB/M machine [13], they are considered suitable for powder processing with regard to the environmental conditions. Since EP is a light-sensitive process, the setup had to be enclosed in a dark box. Each experiment took place without external light. To simulate the step-by-step powder attraction for the intended PBF-LB/M process, two linear axes were implemented for the movement in the x and z-direction. A carrier with a PC is attached to these linear axes to approach the individual process steps. The maximum axis speed of about 300 mm/s and maximum accuracy of 0.3 mm is considered sufficient to describe the initial feasibility of metal powder attraction for PBF-LB/M.

The individual experimental steps in Fig. 4 are defined by the following modules:

(1) Contact charging device, which consists of a soft-foam contact roller that is attached to a variable high voltage (HV) source (iseg HV SHR 4060) and is spring-loaded to achieve a variable contact pressure on the PC (Brother OP 3-CL). This charging procedure induces the time-dependent surface charge parameter (P_{OPC}) on the PC's useable surface for powder attraction [12,13,28].
(2) Electrostatic field measurement sensor (Keyence SK-050) that evaluates the average surface potential on the PC. The surface voltage is measured within a circular area in the center of the PC's useable two-dimensional area (50 mm × 50 mm) for powder attraction. Measurements were taken right after charging to compensate for fluctuations in the achieved surface charge. This reduces the error potential from an overcharged or undercharged PC and enabled adaptive parameter adjustments in further steps.
(3) Static exposure unit based on LED or laser technology which offers variability of beam power with fixed wavelengths.
(4) The powder attraction plate for the metal powder particles out of material of 20MnCr5 with a monomodal PSD between 25 µm and 71 µm. This module was realized as an isolated aluminum plate connected to the HV source, which directly sets the potential (P_{PB}) on the plate's top surface. The attraction takes place directly from the applied powder layer. With the utilized set-up, variable powder layers can be applied within the experimental series. Layer thicknesses were applied up to 4 mm with an increment of 0.01 mm by a continuously adjustable film applicator from BYK-Gardner as well as in fixed heights of 20 mm, 40 mm or 60 mm provided by a frame and filled with powder.
(5) A camera system captured a post-process evaluation image of the attracted powder formation from below the PC. With a digital image processing, images were evaluated for a qualitative attraction coverage but also resulting exposure effects or local coverage errors.

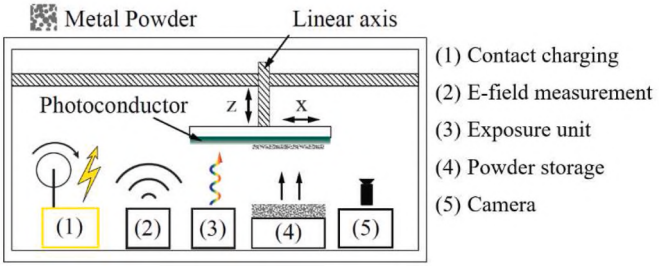

Fig. 4. Schematic representation of the experimental setup and its components.

4. Results and discussion

Two experiments were performed. On the one hand, full-area attraction (Fig. 4 without step 3) and on the other hand selective attraction, which adds the exposure module (Fig. 4 all steps), was investigated. Full-area tests revealed the main parameters and their influences. Hence, these test were intended to show limitations and process reliability. By adding the exposure unit in the process cycle, the powder attraction was considered in terms of the selective powder arrangement required for the practical usage in PBF-LB/M. Selective attraction was a further development of full-area attraction, which was why the experiments are presented from full-area to selective attraction in the further course of this paper.

4.1. Full-area powder attraction

Two scenarios were distinguished in the full-area attraction experiments. One is the attraction of a start layer of around 70 µm on the attraction plate, and the other is the attraction of powder particles with large powder volumes resulting from powder bed thicknesses up to 60 mm. Exemplary images of the experiment with a 70 µm start layer are shown in Fig. 5, where the white parts represent attracted particles. In this experiment series, the attraction was varied in the range from 0.4 MV/m to 0.7 MV/m.

A summary of all performed experiments is shown in Fig. 6. The results indicate that, unlike polymer powders [8], there is no limitation concerning P_{PB} when using 20MnCr5 powder in volumes resulting from powder bed thicknesses up to 60 mm. From a field strength of 0.75 MV/m, a degree of coverage of the PC was determined for both scenarios of powder attraction, which was interpreted as a full-area attraction. The attraction of thin layers was performed in the focus of one of the three main parameters P_{OPC}, P_{PB} and d. With a particularly high surface potential at the surface of the PC as the main driver to reach the field, higher degrees of coverage with a constant coverage increase became apparent in the field transition region. However, the modalities of attraction varied between the individual parameter range and between the thin-layer and powder volume attraction. In the focus of P_{PB} a late-onset and abruptly increasing degree of coverage with an increasing field was observed. Minimizing the distance between OPC and powder bed to 0.1 mm to achieve the necessary field increases for attraction resulted in the worst performance. In addition to the lowest performance

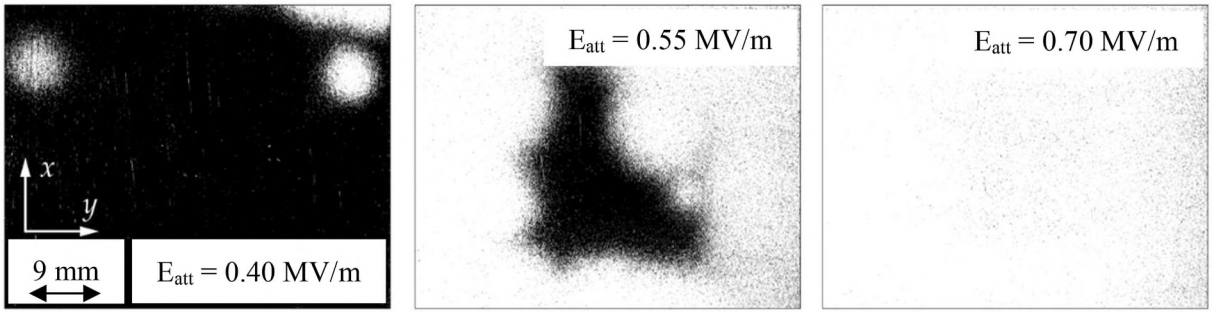

Fig. 5. Images of thin layer attraction with increasing electrostatic field (E_{att}) by raising the potential of the photoconductor.

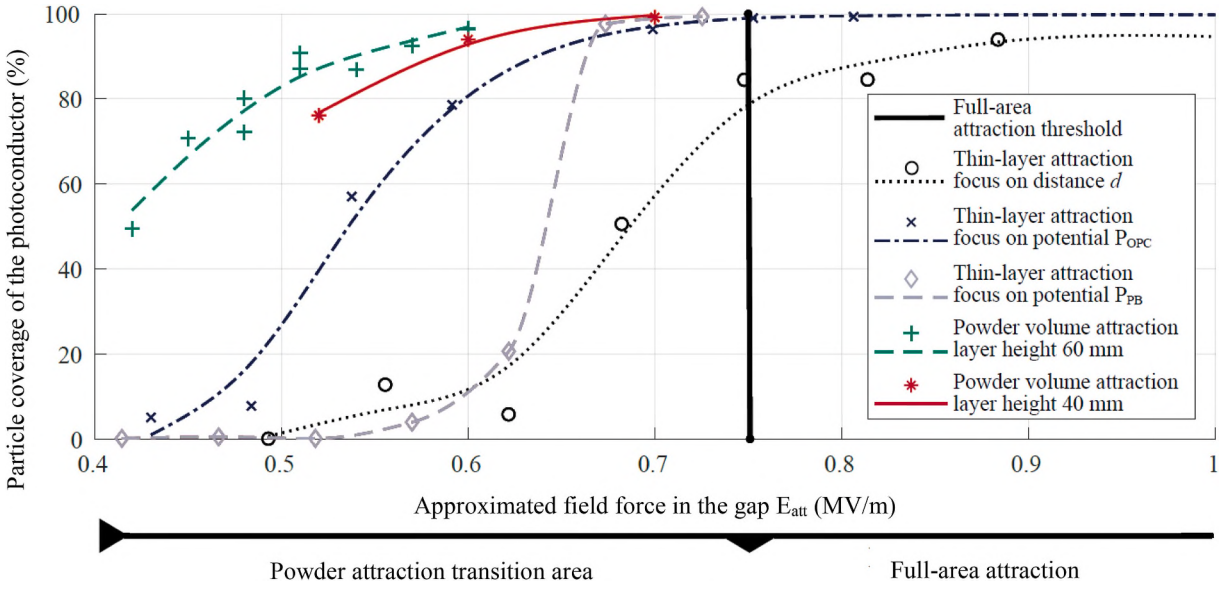

Fig. 6. Results of the full-area attraction.

of attraction, full-field attraction did not occur even for fields above 0.8 MV/m. This may be a process deficit of the used axis system. The low performance suggests that the maximum achievable plane parallelism (0.05 mm) caused fluctuations in the homogeneous field area that induced systematic attraction errors rendering a process-safe attraction impossible. As expected, the influence of the powder permittivity is negligible for the practical attraction of thin layers but significantly determines the process parameters P_{OPC}, P_{PB} and d when it comes to powder volume. Comparing the thin layer attraction with the attraction from the larger powder volumes resulting from powder bed thicknesses of 40 mm and 60 mm, which were achieved with balanced parameter sets for P_{OPC}, P_{PB} and d, it can be seen that the attraction increases with a constant rise in the field strength. Significantly higher degrees of coverage were achieved at fields below 0.5 MV/m than the thin layer attraction. It can be assumed that the offset towards the upper left of the powder volume attraction data points in the diagram in Fig. 6 is a direct result of the approximated field determination via the measured powder permittivity and the consideration of powder as a solid in the underlying capacitor model.

From a practical point of view, the results demonstrate that the powder attraction works reliably and reproducibly with identical maximum coverage levels above the determined field criterion. The achieved degrees of coverage in percent were determined qualitatively among all results by image analysis, but also by mass analysis of the attracted particles. Considering the attracted particle layer as an ideal geometric body with a bulk density of 4.55×10^3 kg/m^3, an average layer height of 30.22 µm was attracted with a field strength of 0.75 MV/m, which seems plausible with the given PSD between 25 µm–71 µm. Measurements conducted with a laser microscope confirmed a maximum achievable layer thickness of up to 65 µm. The obtained layer heights tied directly to the used field strength during attraction. In the next steps, it is necessary to check whether the amount of powder to be attracted can be significantly increased by stronger fields. When increasing the field strength, it must always be considered not to exceed the breakdown voltage of the intended process gas, since metal powder is a combustible material.

4.2. *Static exposure source for selective powder attraction*

An initial potential assessment dealed with a comparison of LED and laser technology. The results of this comparison highlight the potential of different exposure technologies for selective powder attraction. Both exposure sources were selected for the intended use of the photoconductive material, which is the imaging and transfer operation in the laser printing process. The used OPC was designed for a dynamic exposure by a 5 mW near-infrared (NIR) laser diode at 785 nm [29]. The conventional laser is continuously deflected by a scanner unit with rotating polygon mirrors during the intended print operation with up to 600 dpi. Within this work a series of experiments was conducted employing a static exposure unit. To test a dynamic exposure the OPC (attached to the linear axis) traversed the exposure module. The traversing speed was set to 20 – 150 mm/s. Hence, a smaller exposure power of less than 1 mW was assumed sufficient. For the LED source, losses due to diffuse radiation were considered in the power selection. A high-power LED

(Thorlabs M780L3) with a 20°-beam-angle, 780 nm nominal wavelength, and variable output power of up to 200 mW was selected. For uniaxial collimation, the LED was used in a collimation adapter with a cylindrical plano-convex lens. Compact laser diode modules (<1 mW) with acrylic collimator lenses at 650 nm and 780 nm (Roithner Lasertechnik APCD-650-01-C2, APCD-780-01-C2) were used as the laser sources. Although the OPC material was designed for a wavelength of 785 nm [29], it was exposed with 650 nm because it is known that comparable NIR OPCs can still be excited with high sensitivity [24]. The respective exposure source was placed with a variable distance of about 2 mm under the PC and thus represented the process step of exposure. The exposure took place directly after the contact charging of the OPC. The resulting latent charge image on the OPC surface was used in the next step of powder attraction, by analogy with light writing in electrophotography [23], to selectively arrange the powder particles. To evaluate the effects of exposure, the adhering powder on the OPC after attraction was recorded with the camera system. From the images below in Fig. 7, it can be seen that the laser source was superior to the LED source with the utilized system components.

Detail Y indicates the static exposure area during the LED experiment, detail Z the dynamic exposure sweep of the laser focus point during the traverse of the OPC. Despite uniaxial collimation and minor distances between optics and LED of 0.5 mm, unwanted discharge effects as in detail X occurred during LED exposure, preventing the successful selective attraction. Uncontrolled photon scattering could be minimized with the use of an aperture setup, however, even exposure times of 2 s and exploiting the maximum LED power of 200 mW did not yield a reliable powder-free region as exemplified in detail Y. This could still result from further inappropriate focusing of the LED setup. Laser exposure, on the other hand, evoked targeted effects of selective attraction without affecting the surrounding powder attraction. Since areas exposed with laser showed a reduced powder coverage while the remaining semiconductor area was completely covered with powder, this technology was pursued further and is presented in the next section with an optimization approach.

4.3. Optimization of selective powder attraction

The parameters found in section 4.2 were used for selective attraction. Initially, the one-at-a-time method was used to gain insight into the feasibility and provide a basis for further testing. In all experiments, a static exposure module with a laser diode with a wavelength (λ_{exp}) of 650 nm discharged the OPC locally to create a latent, selective surface charge that attracts particles only in the desired unexposed areas. The focal point of the laser was static. The moving carrier with the OPC traversed at constant velocity (v_{exp}) over the focal point with the distance (d_{exp}) between the OPC surface to the laser diode. The traverse induced a dynamic exposure. Before the OPC completely traversed the focal point, the movement was stopped so that the focal point remained at the edge of the OPC for the delay time (t_{exp}) of 2 s until it was switched off to complete the process. This induced a static exposure option. Dynamic exposure was investigated as this is the closest to a real exposure scenario concerning EF. Static exposure, on the other hand, examined and directly visualized the influence of exposure time best. The OPC's dynamic and static exposure regions are indicated in Fig. 8 A.

An incipient exposure effect is already evident from the result shown in sample image Fig. 8 A. For practical application, a powder-free area is required in the exposed areas, so that the exposure effect from image A is not sufficient. It is noticeable in image A that no clear exposure effect occurred even with static exposure. To overcome this deficiency, the internal electrode of the OPC (P_{EL}) was contacted like it is indicated in Fig. 1. Its potential was varied in addition to the previously introduced field parameters P_{OPC}, P_{PB} and d. It was assumed that the electrode potential in combination with the surface charge (P_{OPC}) induces a field in the OPC layer, which favors the efficiency of charge neutralization by photon incidence. With the given parameter selection in Fig. 8 cf. B a successful selective attraction was achieved. As expected, the dynamic exposure influence generated a smaller powder-free area than the static exposure at the edge of the OPC, because of the prolonged photon excitation. This effect highlights the need for faster laser deflections for future exposure systems capable of generating relevant selective attracted powder patterns for additive manufacturing. Further examinations in Detail W show a sharp transition of 0.2 mm. Furthermore, Detail W reveals that the powder-free area is not completely free of particles. According to the analysis of the image evaluation, on average, about 24 particles remained per square centimeter.

To further optimize the exposure results and quantify the effects, a statistical design of experiments (DOE) approach was used. A quadratic D-optimal experimental design with 100 parameter-varying iterations was performed. In addition to the parameters P_{EL}, P_{OPC}, P_{PB} and d_{exp} that exist purely from the process of powder attraction, there are several application-related exposure parameters within the framework of laser exposure. The exposure speed and distance are specific parameters of the exposure source such as wavelength, beam power, and beam distribution and focusability. In the experiment, the dynamic laser exposure was tested exclusively. The potential parameters (P_{EL}, P_{OPC}, P_{PB}), the exposure speed (v_{exp}) and distance (d_{exp}) as well as the diode voltage (U_{laser}) for beam power variation act as factors. The value intervals used for the significant parameters can be seen in Fig. 9. Parameter combinations that resulted in an insufficient field for attraction (e. g. resulting from potentials of P_{OPC} and P_{PB} below the given values) were not considered in the evaluation. The two target values were: Firstly the

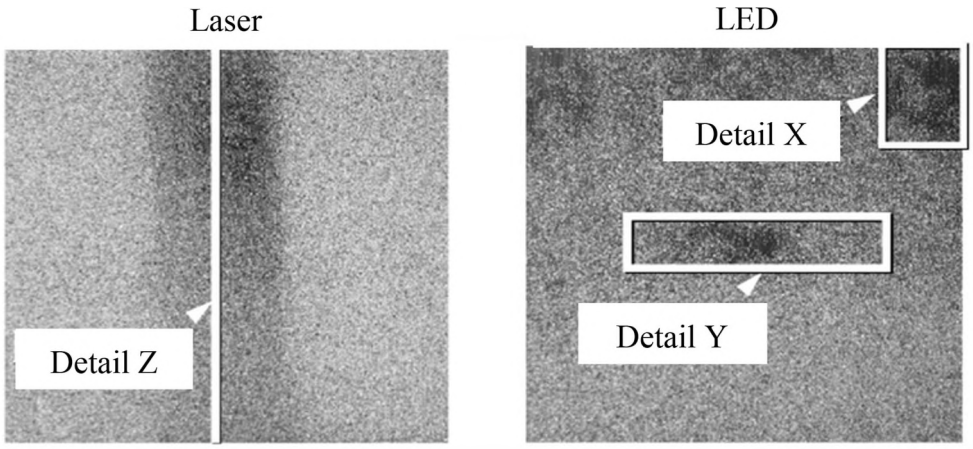

Fig. 7. Comparison of static exposure units for selective powder attraction.

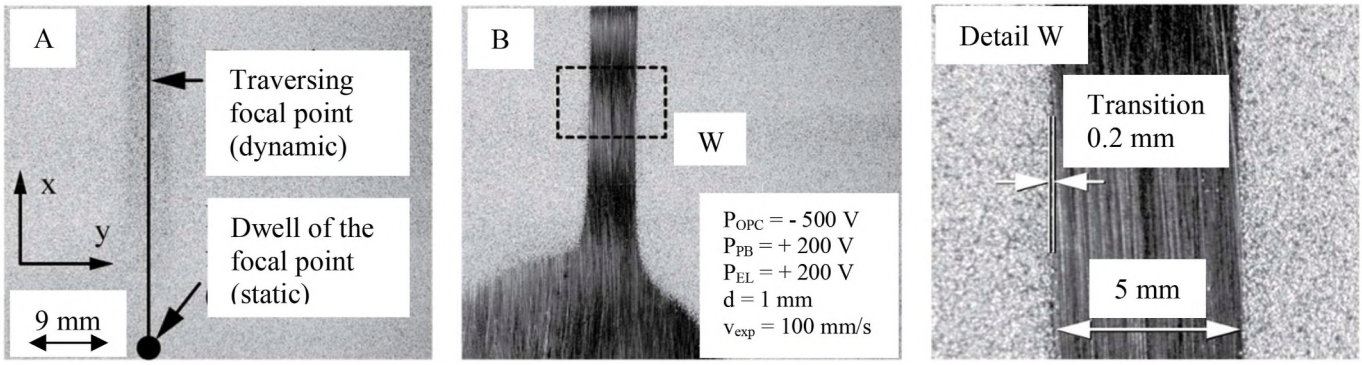

Fig. 8. Captured results for selective powder attraction.

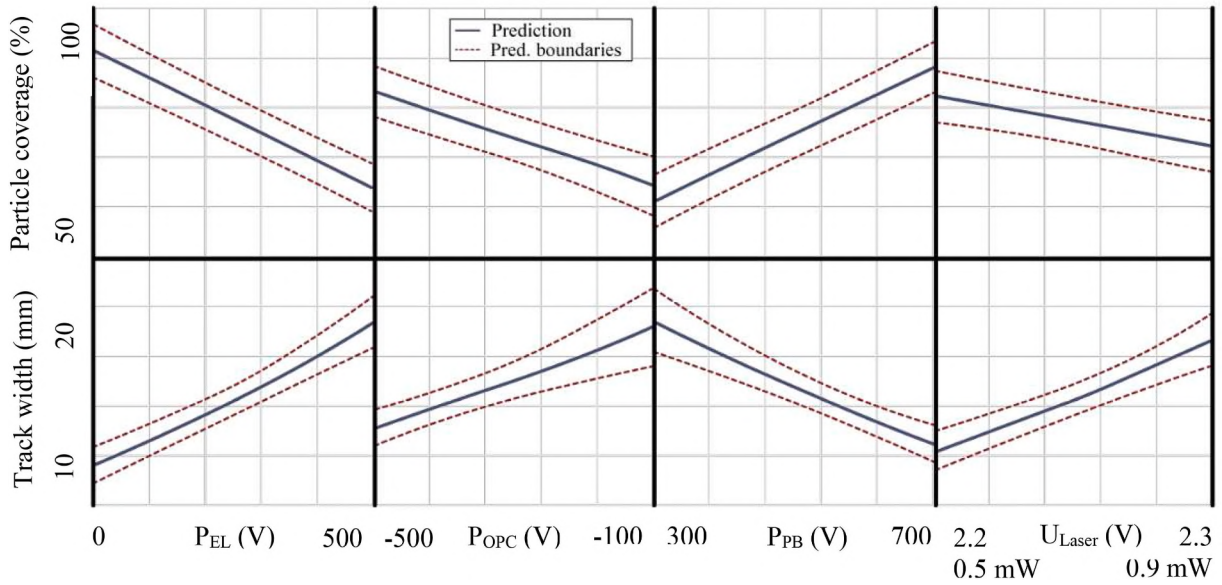

Fig. 9. Prediction of the influences of significant parameters during exposure at wavelength of 650 nm based on software evaluation. The factors of vexp and dexp did not show a significant influence. The considered values were V_{exp} = [40; 60] mm/s and d_{exp} = [21,4] mm.

qualitative particle coverage of the OPC in percent reaching a quality criterion R^2 of 82.9%. And secondly the detected track width (R^2 of 76.7%) of the powder-free area as a result of the dynamic exposure identical to Detail W (cf. Fig. 8). The different parameter combinations led to different field forces around 0.75 MV/m. The experiment led to a statement about the effects of relevant parameters. The exposure speed and the distance had no significant exposure effect so they were removed from the model to assign their degrees of freedom to the model error. Further, there were no significant quadratic effect terms or higher-order interactions. The analysis of the parameter interaction showed no practical relevant interactions between the remaining parameters. The evaluation of the particle coverage showed a higher model quality as the manually measured track width as a consequence of the underlying automated software evaluation. This directly led to coarser prediction bands in the track width prediction. Here, a comparison between the track width and the particle coverage offers a further validation angle, since the effect in the diagram must be contrary. In addition to the shown tendencies, the significance order of the parameters was determined as follows: $P_{PB} > P_{OPC} > P_{EL} > U_{Laser}$. Each parameter behavior can be seen in the resulting prediction diagram in Fig. 9.

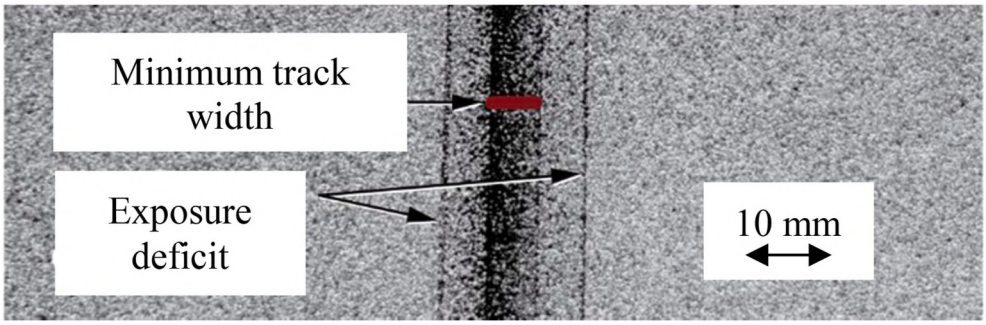

Fig. 10. Process deficit in the exposure of track widths below 5 mm.

The optimization of the parameter sets to the minimum possible track width revealed new challenges in the system used. The resulting parameter sets led reproducibly to uncontrolled exposure deficit phenomena close to the powder-free region as shown in Fig. 10. This unwanted exposure deficit could be due to issues regarding the integrated optics or unsuitable beam characteristics. For subsequent tests, higher grade laser diodes with a focus ability below 0.1 mm and with precision optics with tail-free top-hat distribution might be an option for further improvements.

The results on the selective attraction by exposure show important influences for the further development of the recoating system. So far, it is not explained why the speed of the exposure does not show a significant influence. In the case of the velocity parameter, it is assumed that high speeds cannot be transferred linearly to the exposure effect due to the necessary acceleration and braking operations of the axis system. For fields above 0.75 MV/m the exposure effect was increasingly reduced. If exposure for such strong fields is required, a more field-strength-independent effect would be beneficial. For this purpose, it may be useful to disconnect the OPC with the selective latent charge pattern from all electrical connections just prior to attraction, as the image would then be in an isolated state right before the particle attraction It should be noted that with the utilization of moderate traversing speeds and a static laser diode, a track width smaller than 5 mm cannot be realized. However, the practice of additive component manufacturing requires resolutions from e. g. 0.6 mm [30]. Research efforts need to clarify whether fast-deflected laser diodes can produce these filigree charge patterns that will correspond to the desired layer arrangement after attraction and deposition with a certain tolerance.

5. Conclusion

In this paper, the electrostatic attraction ability of the gas atomized steel powder 20MnCr5 (1.7147) has been investigated on an OPC using the EP principle. The metallic powder represents a typical alloy processed by laser-based powder bed fusion. The investigation was aimed at the sequential development of an EP powder application module for powder bed fusion of metals using a laser beam and, in perspective, for other powder bed-based additive manufacturing processes. Two scenarios were considered: First, full-area and second, selective powder attraction to the OPC. The possibility of full-area attraction by electrostatic field forces from powder storages, as used in many PBF-LB/M systems, could be demonstrated starting from layers of the powder bed with 70 µm up to powder beds with a thickness of 60 mm. For the selection of the process parameters for the full-area powder attraction, the electrostatic field between the OPC as well as the powder on the powder bed was considered via simulation, taking into account the geometric conditions. In theory, a field of at least 0.3 MV/m should be sufficient for the attraction of the steel powder under atmospheric conditions. In the experimental investigations, the process-safe full area coverage was identified from 0.75 MV/m. Therefore, it can be assumed that the ideal, theoretical assumptions for parameter determination are subject to further influences that have not yet been investigated in this context. Besides the Coulomb force, additional atomic-level force influences such as image charges of the particles and interactions due to van der Waals surface forces are considered likely. Furthermore, insufficient charging of the particles in the powder bed or agglomeration mechanisms not considered so far could lead to an increase of the required field force. For reproducible attraction, the process parameters of the potential at the powder bed and the surface potential at the OPC showed the strongest influence. Considering undesired field-induced particle movements, the OPC potential should be maximized first and then the powder bed potential. Moreover, in the simulative investigation, fringing fields were identified. These are not to be classified as critical for powder attraction with the field forces used, but which can be expected to influence the further process for depositing the powder. The extent to which higher field forces can increase the powder coverage from full-area powder attraction without process deficits must be investigated further in the future.

For a first selective attraction, LED and laser diodes of wavelengths 650 nm and 780 nm were compared with respect to their reproducible exposure result on the OPC. In the given setup, the laser diodes showed a reproducible discharge of the OPC superior to the LED source. This discharge leads to the successful selective attraction of powder to the OPC. In a focused parameter study on the exposure process, it was shown that the effect of the process parameters can be compared with each other as follows: $P_{PB} > P_{OPC} > P_{EL} > U_{Laser}$. Accordingly, the potential at the powder bed has the greatest influence on the exposure result. An important indicator of the system's ability to generate the finest powder patterns for additive manufacturing is the achievable track width during selective attraction. So far, a track width of less than 5 mm is not feasible with the given setup and its partially static components. In the future, the track width could be minimized by focusing the laser spot diameter to at least 0.1 mm and by applying faster deflection times.

Declaration of competing interest

The authors declare that they have no known competing financial interests or personal relationships that could have appeared to influence the work reported in this paper.

Acknowledgments

The authors express their sincere thanks to the State of Bavaria and its Bavarian Ministry of Economic Affairs, Regional Development and Energy StMWi for funding the "MULTIMATERIAL-Zentrum Augsburg" (English: "Multi-material Center Augsburg").

References

[1] Wohlers Associates: WOHLERS Report, 3D Printing and Additive Manufacturing, Global State of the Industry, 2020, pp. 50–90.
[2] S. Girnth, J. Koopmann, G. Klawitter, et al., 3D hybrid-material processing in selective laser melting: implementation of a selective coating system, Prog. Addit. Manuf. 4 (2019) 399–409. Nr. 4.
[3] M. Ott, Multimaterialverarbeitung bei der additiven strahl- und pulverbettbasierten Fertigung, Herbert Utz Verlag, 2012.
[4] C. Seidel, C. Anstätt, Next step in laser-based powder bed fusion - multi material processing, Laser Technik J. 13 (2016).
[5] G. Lanzar, et al., Laser-Strahlschmelzen - Technologie mit Zukunftspotenzial. Ein Handlungsleitfaden, Karlsruher Institut für Technologie Institut für Produktionstechnik, 2017.
[6] A.V. Kumar, A. Dutta, J.E. Fay, Electrophotographic printing of part and binder powders, Rapid Prototyp. J. 10 (2004) 7–13.
[7] T. Stichel, T. Laumer, P. Amend, et al., Electrostatic Multi-Material Powder Deposition for Simultaneous Laser Beam Melting, Erlangen, 2014.
[8] A.V. Kumar, Z. Hongzin, Electrophotographic Powder Deposition for Freeform Fabrication, 1999, pp. 1–8.
[9] K. Boivie, R. Karlsen, C. Van der Eijk, Material Issues of the Metal Printing Process, MPP, 2006, pp. 197–208.
[10] K. Boivie, R. Karlsen, O. Åsebø, The Metal Printing Process; the Development of a New Additive Manufacturing Process for Metallic Materials, Swedish Production Symposium, 2008.
[11] K. Boivie, R. Karlsen, C. Van der Eijk, O. Åsebø, Issues of Incremental Graded Metallic Materials by the Metal Printing Process, MPP. Additive Layered Manufacturing from Evolution to Revolution, 2008.
[12] J. Förster, M. Michatz, et al., Aspects of Developing a Powder Application Module Based on Electrophotography for Additive Powder Bed Based Processes, Machining Innovations Conference for Aerospace Industry, 2020, pp. 147–152.
[13] P. Kindermann, M. Michatz, J. Förster, et al., Technological Potential of Electrostatics for Powder Bed Fusion Processes, EuroPM Congress&Exhibition, 2019.
[14] M. Binder, C. Anstaett, M. Horn, et al., Potentials and challenges of multi-material processing by laser-based powder bed fusion, Solid Freeform Fabr. 29 (2018) 376–387.
[15] S. Vock, B. Klöden, A. Kirchner, et al., Powders for Powder Bed Fusion: A Review. Progress in Additive Manufacturing, 2019.
[16] A. Gebhardt, Generative Fertigungsverfahren, Hanser Verlag, 2013, pp. 59–66, 66-68.
[17] C. Anstaett, C. Seidel, G. Reinhart, Multi-material processing in laser beam melting, in: Direct Digital Manufacturing Conference, 2016.

[18] C. Anstaett, C. Seidel, G. Reinhart, Herstellung von 3-D-Multimaterialbauteilen aus Kupfer-Chrom-Zirkonium und Werkzeugstahl 1.2709, Rapid.Tech Fachkongress (2018).
[19] C. Anstaett, C. Seidel, Multi-Material Processing. Next step in laser-based powder bed fusion, Laser Technik J. (2016).
[20] M. Michatz, A. Frey, J. Förster, et al., Electrostatic Modelling of a Particle Application Module for Additive Manufacturing, Comsol Congress, 2019.
[21] K. Bammel, Organisch kopiert, Phys. J. 2 (2006) 42–43.
[22] A.S. Diamond, D.S. Weiss, Handbook of Imaging Materials, Marcel Dekker, New York, 2002.
[23] G. Goldmann, Das Druckerbuch. Technik und Technologien der OCÉ-Drucksysteme, 2002, pp. 85–90.
[24] D. Weiss, M. Abkowitz, S. Kasap, , et al.Hrsg, Handbook of Electronics and Materials, Organic Photoconductors, 2017.
[25] K.H. Herrmann, Der Photoeffekt, Grundlagen der Strahlungsmessung. Vieweg&Sohn, 1994.
[26] B. Morgenstern, Elektronik 1, Springer, 1993.
[27] B. Techaumnat, S. Matsusaka, Effect of charge transfer on electrostatic adhesive force under different conditions of particle charge and external electric field, Powder Technol. 301 (2016) 153–159.
[28] H. Hirakawa, Y. Murata, Mechanism of contact charging photoconductor and insulator with DC-biased conductive roller, in: IAS '95. Conference Record of the 1995 IEEE Industry Applications Conference Thirtieth IAS Annual Meeting, Orlando, FL, USA, 1995, pp. 1539–1542.
[29] Brother, Brother Color Laser Printer SERVICE MANUAL, 2001. Modell HL-2600CN.
[30] M. Binder, M. Illgner, G. Schlick, C. Seidel, et al., Laser Beam Melting of Complexly Shaped Honeycomb Structures, Technologies for Lightweight Structures (TLS), 2018.